PAPER

Check for updates

Investigating the enhancement of the rate of CO_2 capture of CaO in the presence of steam through ^{18}O isotope labeling: pitfalls and findings

Felix Donat [ID] * and Christoph R. Müller [ID] *

The reaction of CO_2 with CaO to form $CaCO_3$ can be used to remove CO_2 from gas streams in post-combustion CO_2 capture schemes at high temperatures (>600 °C). The rate of CO_2 uptake is increased substantially in the presence of steam, but the underlying reasons have not yet been resolved, although several explanations have been proposed in the literature. In our study we generated steam from labeled water ($H_2^{18}O$) to track ^{18}O in the gas and solid products using mass spectrometry and Raman spectroscopy, aiming to understand whether oxygen (or OH^-) contained in H_2O participates directly in the formation of $CaCO_3$. Unfortunately, it was not possible to investigate the interaction of $H_2^{18}O$ with $CaO/CaCO_3$ isolated, because in the presence of CO_2 oxygen was exchanged between H_2O and CO_2 in the high-temperature reaction chamber of the thermogravimetric analyzer before any interaction of the gaseous reactants with the sorbent. ^{18}O was detected in the $CaCO_3$ product, but it originated from ^{18}O in CO_2 rather than H_2O. Yet, our measurements suggest that oxygen exchange occurs between CaO and H_2O under reaction conditions, but not between $CaCO_3$ and H_2O/CO_2, which may motivate further investigations.

1. Introduction

Calcium looping is a promising technique to capture CO_2 from point sources at high efficiency.[1–3] On a process level, CaO-based sorbents react with CO_2 contained in flue gases from combustion or other CO_2 emitting processes at temperatures between 600 and 700 °C (carbonation), removing up to 90% of the CO_2.[4–6] The resulting $CaCO_3$ is decomposed subsequently at a high temperature (>900 °C) to release CO_2 and recover the CaO-based sorbent (calcination). The CO_2 obtained from the decomposition of $CaCO_3$ can be compressed and stored underground, or used as a feedstock in chemical conversion processes.[7,8] CaO-based sorbents tend to lose their activity for fast CO_2 sorption with increasing number of cycles of CO_2 sorption and release. The high theoretical CO_2 uptake capacity of 0.78 g CO_2 per g CaO is practically not achievable owing to sintering that reduces surface area and pore volume.[3] During carbonation, CO_2 molecules need to diffuse through a network of narrow pores within the sorbent particle, and as pores close due to the built-up of the product $CaCO_3$, the rate of CO_2 sorption decreases; some of the CaO contained in the sorbent particle is not even accessible for CO_2 at all within typical residence times.

Interestingly, small quantities of steam (even <1 vol%) present in the CO_2-containing gas increase the rate of CO_2 sorption of CaO (*viz.*, the rate of $CaCO_3$ formation).[9] The increase is most significant when intraparticle diffusion controls the rate of CO_2 sorption, indicating that steam influences the diffusional transport of CO_2 within the sorbent. Steam is also known to accelerate the decomposition of $CaCO_3$ (ref. 10–13) and affect the structural and morphological properties of the CaO formed,[11,14,15] resulting sometimes even in an increase in mechanical strength.[16,17] It has been observed that the CO_2 uptake of limestone-derived CaO was improved under dry conditions when the decomposition of $CaCO_3$ in the previous reaction step was performed in the presence of steam, because the resulting pore structure of CaO was more favorable for fast CO_2 sorption, offering less intraparticle diffusional resistance for CO_2 molecules.[9,18]

Despite numerous studies, the mechanism of the enhancing effect of steam during CO_2 sorption at high temperatures (>600 °C) is still not fully understood. An overview of relevant investigations concerning the effect of steam on the carbonation reaction has been provided recently by Dunstan *et al.*,[3] building up on earlier work by Zhang *et al.*[19] Several studies have hypothesized that OH^- groups originating from the dissociative adsorption of steam on the surface of CaO play an important role,[20,21] but no experimental evidence has been provided yet; note that the phase $Ca(OH)_2$ is thermodynamically not stable at ambient pressure at temperatures >550 °C, and is therefore not expected to contribute as an intermediate species to the faster CO_2 sorption. Coverage of the CaO surface with OH^- would not explain why the enhancement of the rate of CO_2 sorption is

Laboratory of Energy Science and Engineering, Department of Mechanical and Process Engineering, ETH Zürich, Leonhardstrasse 21, 8092 Zürich, Switzerland. E-mail: donatf@ethz.ch; muelchri@ethz.ch

most noticeable once a significant amount of CaO has been converted into $CaCO_3$ already. Li et al.[22,23] proposed a mechanism that considers diffusional transport in the $CaCO_3$ product layer: H_2O molecules dissociate on the $CaCO_3$ surface (gas–solid interface), forming H^+ and OH^-. Given the small radius of H^+, it diffuses rapidly through the $CaCO_3$ product to the CaO–$CaCO_3$ interface, where it reacts with O^{2-} to form OH^-. OH^- diffuses outwards to the $CaCO_3$–gas interface to react with CO_2, forming CO_3^{2-} that diffuses inwards through the $CaCO_3$ product layer to the CaO–$CaCO_3$ interface, where new $CaCO_3$ is ultimately formed. OH^- diffusion is faster than O^{2-} diffusion under dry conditions and so is assumed to explain the increase in the rate of $CaCO_3$ formation in the presence of steam; note that the counter-current diffusion mechanism of CO_3^{2-} and O^{2-} under dry conditions was experimentally demonstrated by Sun et al.[24] through an inert marker experiment. Strictly speaking, it is not the OH^- on the surface (which originates from the dissociation of H_2O) that participates in the formation of $CaCO_3$, but the OH^- formed following proton (H^+) diffusion and reaction with O^{2-}. This is different from recent density functional theory (DFT) results to understand the promotion of CO_2 sorption on Li_4SiO_4-based sorbents with water vapor, which conclude that surface OH^- contributes to the enhanced CO_2 uptake.[25]

An interesting body of literature deals with the diffusion of oxygen, hydrogen and carbon in minerals (including the calcite polymorph of $CaCO_3$), relevant to many geological processes such as fluid–rock interactions or the growth of minerals.[26] Using isotope tracers such as ^{18}O or ^{13}C and ion microprobes, it was found that volume/lattice diffusion of oxygen is improved substantially (by at least 1–2 orders of magnitude) in the presence of water, whereas carbon and cations diffusion are hardly affected by the presence of water (400–800 °C, total pressure 0.1–350 MPa).[27,28] In many types of minerals such as quartz, feldspars and calcite, molecular H_2O rather than OH^- was identified as the dominant diffusing species bearing oxygen under hydrothermal conditions, as oxygen transport depended linearly on water fugacity.[29–31] The rate of diffusion of oxygen is believed to be controlled by reactions at the surface of calcite,[32,33] which may be relevant also for typical calcium looping conditions. Specifically, adsorption of H_2O and the creation of vacancy defects at the surface explain the dependence of the diffusivity of oxygen on the fugacity of water. The dissociation of water on the calcite surface supplies protons that hydrolyze and weaken C–O bonds in calcite akin to Si–O bonds in silicates, and thus makes oxygen exchange between H_2O and structurally bound oxygens energetically favorable.[30,32] Carbonate ion (CO_3^{2-}) was identified as the dominant carbon-containing diffusing species in calcite from measurements of the oxygen/carbon exchange rate ratio.[34] Furthermore, there has been little evidence that hydrogen itself diffuses into calcite, and it has been concluded that hydrogen cannot be responsible for the increased diffusivity of oxygen in calcite.[32]

In this work, we investigate whether oxygen contained in steam (or OH^- groups originating from steam) is involved directly in the formation of the $CaCO_3$ product. Such involvement (or non-involvement) would shed light on the sequence of reactions that lead to $CaCO_3$ formation, and help understand

whether steam contributes to the increased rate of CO_2 uptake as a carrier of oxygen. Thus, we co-feed steam containing the oxygen isotope ^{18}O (i.e., $H_2^{18}O$) during the carbonation reaction, use Raman spectroscopy to detect ^{18}O in the $CaCO_3$ formed, and mass spectrometry to detect ^{18}O in the CO_2 released from the $CaCO_3$.

If, as proposed by Li et al.,[23] OH^- groups originating from the reaction of H^+ (from the dissociation of $H_2^{18}O$) with O^{2-} at the CaO–$CaCO_3$ interface interact with CO_2 molecules and form CO_3^{2-}, then any CO_2 released during the decomposition of $CaCO_3$ should not contain ^{18}O because the origin of O^{2-} is not the $H_2^{18}O$ molecule. If, however, oxygen or OH^- groups from $H_2^{18}O$ on the surface of CaO/$CaCO_3$ (the solid–gas interface) participate in the formation of CO_3^{2-}, then the CO_2 released during the decomposition of $CaCO_3$ should indeed contain ^{18}O, e.g., as $C^{16}O^{18}O$ or $C^{18}O^2$. Generally, any indication of ^{18}O in the CO_2 released from the sorbent (beyond their natural abundance) would imply that steam participates actively in the formation of $CaCO_3$ rather than acting as a catalyst or functioning by other means; this would also disprove the mechanism proposed by Li et al. as the only pathway by which steam enhances the rate of CO_2 sorption/$CaCO_3$ formation. Not detecting ^{18}O in the CO_2 released from the decomposition of $CaCO_3$ would not directly prove the mechanism proposed by Li et al. but demonstrate that oxygen or OH^- groups originating from steam do not contribute to the formation of CO_3^{2-} and $CaCO_3$.

2. Experimental materials and methods

2.1 CaO-based sorbent

Natural limestone (Rheinkalk, >98 wt% $CaCO_3$, surface area ∼1 $m^2 g^{-1}$) was used in all experiments as the precursor for CaO. Prior to the experiments using a thermogravimetric analyzer (TGA), limestone particles were calcined at 900 °C in N_2 for 30 min, followed by cooling to room temperature. The sorbent particles were then sieved to 150–212 μm to ensure that in the TGA experiments their packing inside the crucible had no influence on the CO_2 transport that would otherwise affect the observed rate of CO_2 uptake.[35]

2.2 Material characterization

Raman spectroscopy on powdery, partially carbonated samples was performed using a Thermo Scientific DXR Raman microscope (laser wavelength 455 nm). The crystalline phases of the powdery samples were analyzed via X-ray diffraction (XRD) using a PANalytical Empyrean X-ray diffractometer (Cu Kα radiation, 45 kV and 40 mA) equipped with a X'Celerator Scientific ultrafast line detector and Bragg–Brentano HD incident beam optics.

2.3 Thermogravimetric analyzer (TGA) setup

CO_2 sorption experiments were carried out using a TGA (Mettler Toledo, TGA/DSC1, volume of the high-temperature reaction chamber: 16 ml) following the same principal protocol: sorbent

particles (15–20 mg) were loaded into a shallow, 30 µl crucible made of aluminum oxide and heated to 900 °C in N_2. After 15 min, the temperature was reduced to 650 °C (CO_2 sorption temperature). The gas atmosphere was changed from pure N_2 to 15 vol% CO_2/N_2 for 20 min for CO_2 sorption in the presence or absence of steam. 15 vol% CO_2/N_2 was used to reflect typical CO_2 concentrations in post-combustion CO_2 capture, and enable comparison with previous works. Subsequently, the gas atmosphere was changed back to N_2, and the temperature was increased to 950 °C (CO_2 release temperature). After holding at 950 °C for 10 min, the temperature was decreased to 650 °C for a new reaction cycle to begin. Note that only the CO_2 sorption stage was performed in the presence of steam, but not the heating, cooling and CO_2 release stages. Heating and cooling rates were 30 °C min^{-1} and the total flow rate was always 100 ml min^{-1} (incl. 25 ml min^{-1} of dry N_2 purge over the micro-balance), as measured and controlled at normal temperature and pressure by mass flow controllers (Bronkhorst, EL-FLOW).

Steam was generated by flowing 60 ml min^{-1} of N_2 (or 60 ml per min N_2 and 15 ml per min CO_2, see details below) through a small gas washing bottle (volume 5 ml) filled with deionized water or water containing the isotope ^{18}O (labeled water, $H_2^{18}O$, 97 atom% ^{18}O, Sigma-Aldrich) at ambient temperature, as shown in Fig. 1. Separate measurements using a humidity probe (Sensirion, SHT31) showed ~90% saturation of the gas stream with water. The temperature of the laboratory (and the water in the gas washing bottle) varied between 22 and 24 °C, and hence the steam concentration in the reaction chamber of the TGA was ~1.5–2.0 vol% (a larger flow rate through the saturator and a higher ambient temperature result in a higher steam concentration). A solenoid valve synchronized with the temperature program of the TGA enabled the sharp separation of dry and humid gas environments. In addition to the two types of water used (deionized water or water containing the isotope ^{18}O), two options for mixing CO_2 and steam/water prior to entering the TGA reaction chamber were investigated (Fig. 1). The first option aimed at mixing CO_2 and steam in the gas phase; thus, pure N_2 flowed through the saturator and was mixed with the CO_2 stream after the saturator just before entering the reaction chamber of the TGA. For the second option, a mixture of N_2 and CO_2 flowed through the saturator, such that also CO_2 was mixed with liquid water to generate steam; this option was always used when deionized water was used.

The gas outlet from the TGA was connected directly to a mass spectrometer (MS, MKS Cirrus 3) through a heated transfer line

Table 1 Relative intensities of the different mass-to-charge ratios (m/z) for the relevant gas species[36]

Mass-to-charge ratio (m/z)	Species					
	$H_2^{16}O$	$H_2^{18}O$	$^{16}O_2$	$C^{16}O_2$	$C^{16}O^{18}O$	$C^{18}O_2$
18	100	n/a	0	0	n/a	n/a
20	0.3	100	0	0	n/a	n/a
32	0	0	100	0	n/a	n/a
44	0	0	0	100	n/a	n/a
46	0	0	0	0.4	100	n/a
48	0	0	0	0	n/a	100

to analyze the composition of the product gases, and to detect ^{18}O in CO_2 and H_2O (see Table 1). When changing the atmosphere from 15 vol% CO_2/N_2 to pure N_2 after the CO_2 sorption stage, the release of CO_2 from the sample did not occur immediately, but required higher temperatures (>700 °C) for kinetic reasons. The MS was sufficiently fast to resolve the two events of (i) a decreasing CO_2 signal due to the change in atmosphere from 15 vol% CO_2/N_2 to pure N_2, and (ii) an increasing CO_2 signal due to the release of CO_2 from the sample during the decomposition reaction when heating to 950 °C.

3. Results

3.1 TGA cyclic performance and MS signals

Fig. 2a and b compare the normalized sample mass of the limestone-based sorbent under dry and humid conditions over five cycles of CO_2 sorption and release. A value of one implies that the sorbent is calcined completely, and any increase in normalized sample mass is due to the sorption of CO_2 when the material transitions from CaO to $CaCO_3$. The difference between the normalized sample mass and one is thus equivalent to the CO_2 uptake in g CO_2 per g sorbent, and it can reach a maximum value of ~0.77 for this particular sorbent for the case that all CaO is converted into $CaCO_3$ (the normalized sample mass would then show a value of 1.77).

Under dry conditions, the CO_2 uptake observed at the end of the CO_2 sorption stage decreased gradually with cycle number, as is commonly observed for limestone-based sorbents.[37] Under humid conditions, the CO_2 uptake was significantly higher and even increased slightly with cycle number. Whether deionized water, labeled water, or a mixture of deionized and labeled water was used during carbonation did not affect the observed rate and extent of the CO_2 uptake during the five cycles of CO_2
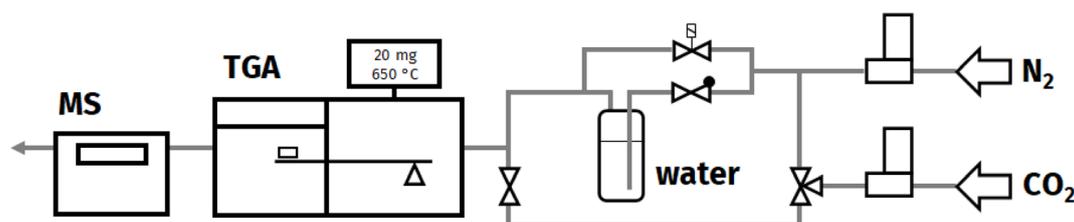

Fig. 1 Schematic illustration of the experimental setup using TGA and MS, and the steam injection system.
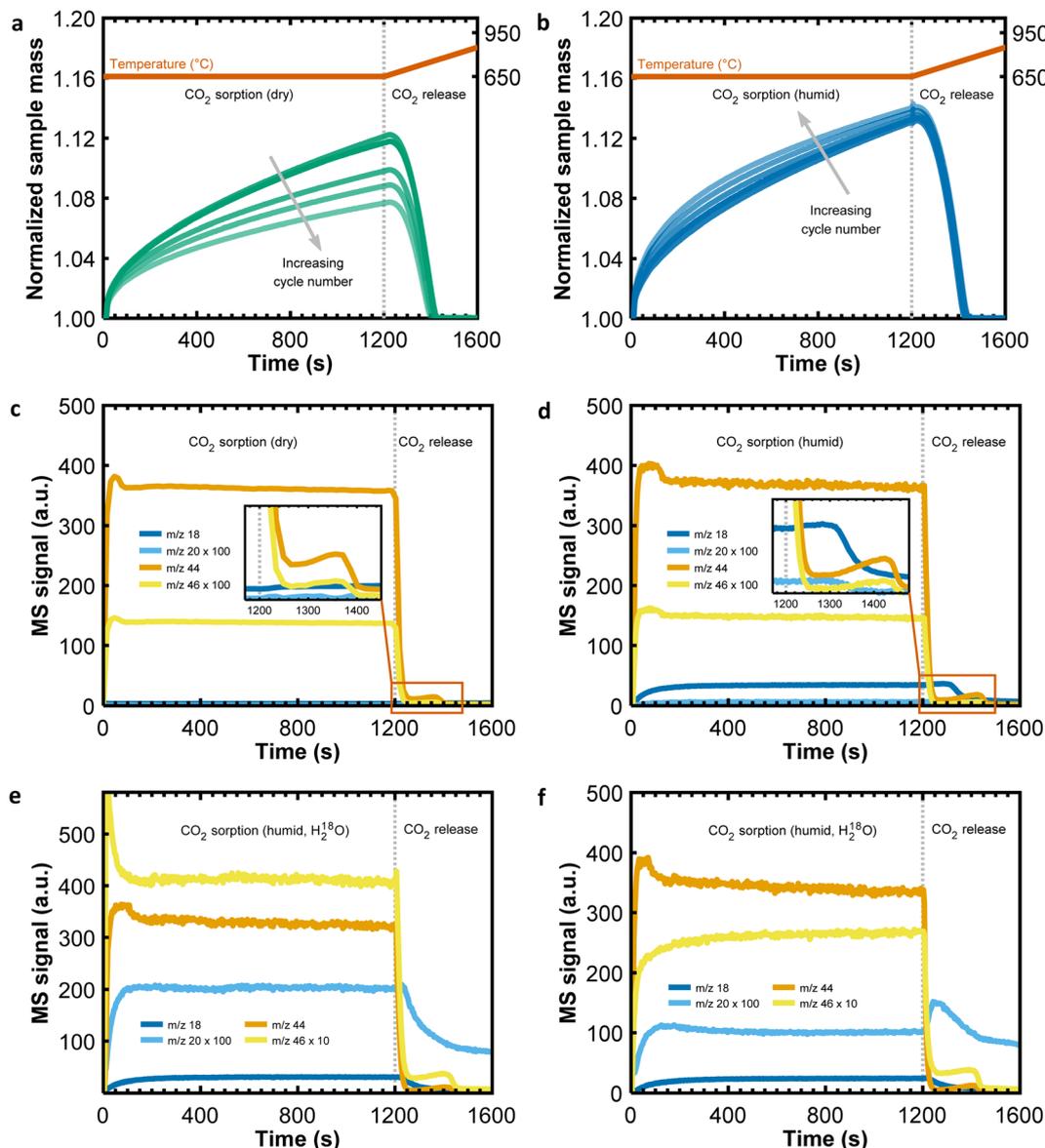
© 2025 The Author(s). Published by the Royal Society of Chemistry

Fig. 2 Results from the TGA experiments over five cycles of CO_2 sorption and release using a limestone-based sorbent. (a) CO_2 sorption in a dry CO_2-containing atmosphere. (b) CO_2 sorption in a humid CO_2-containing atmosphere using deionized water. (c) and (d) Show the MS signals corresponding to the TGA measurements shown in (a) and (b) for the fifth carbonation cycle. (e) and (f) Show the MS signals that correspond to the same cycling experiment shown in (b), but using steam derived from labeled water ($H_2^{18}O$) instead of deionized water; in (e) both N_2 and CO_2 flowed through the saturator, whereas in (f) only N_2 flowed through the saturator.

sorption and release (supplementary plots in Fig. 4a and b). Also, small variations in the steam concentration (due to minor temperature variations in the laboratory, the different flow rates of gas through the saturator, or the water level in the saturator) had no noticeable effect on the observed CO_2 uptake. Adding steam to the CO_2-containing atmosphere during the CO_2 sorption stage increased the rate of CO_2 sorption even after a substantial amount of $CaCO_3$ had been formed already under dry conditions (shown below in Fig. 4c). From Fig. 2a and b it is apparent that CO_2 was released from the sorbent before the CO_2 release temperature of 950 °C was reached, but whether steam was present during the CO_2 sorption stage or not did not affect the rate of the subsequent decomposition of $CaCO_3$ noticeably.

Fig. 2c and d plot the MS signals under dry and humid conditions, respectively, recorded during the fifth reaction cycle, whereas Fig. 2e and f show the MS signals recorded during the fifth reaction cycle when labeled water ($H_2^{18}O$) instead of deionized water ($H_2^{16}O$) was used to generate steam; note that the MS signals are plotted on a linear scale and that the intensity of some signals (*e.g.*, m/z 20 or m/z 46) was magnified for illustration purposes. Under dry conditions (Fig. 2c) signals due to CO_2 (m/z 44 and 46) were observed, whereas in the presence of unlabeled steam (containing only ^{16}O, Fig. 2d) also signals due to H_2O (m/z 18 and 20) were observed. When changing the atmosphere from (dry or humid) 15 vol% CO_2/N_2 to pure N_2 at the end of the carbonation stage,
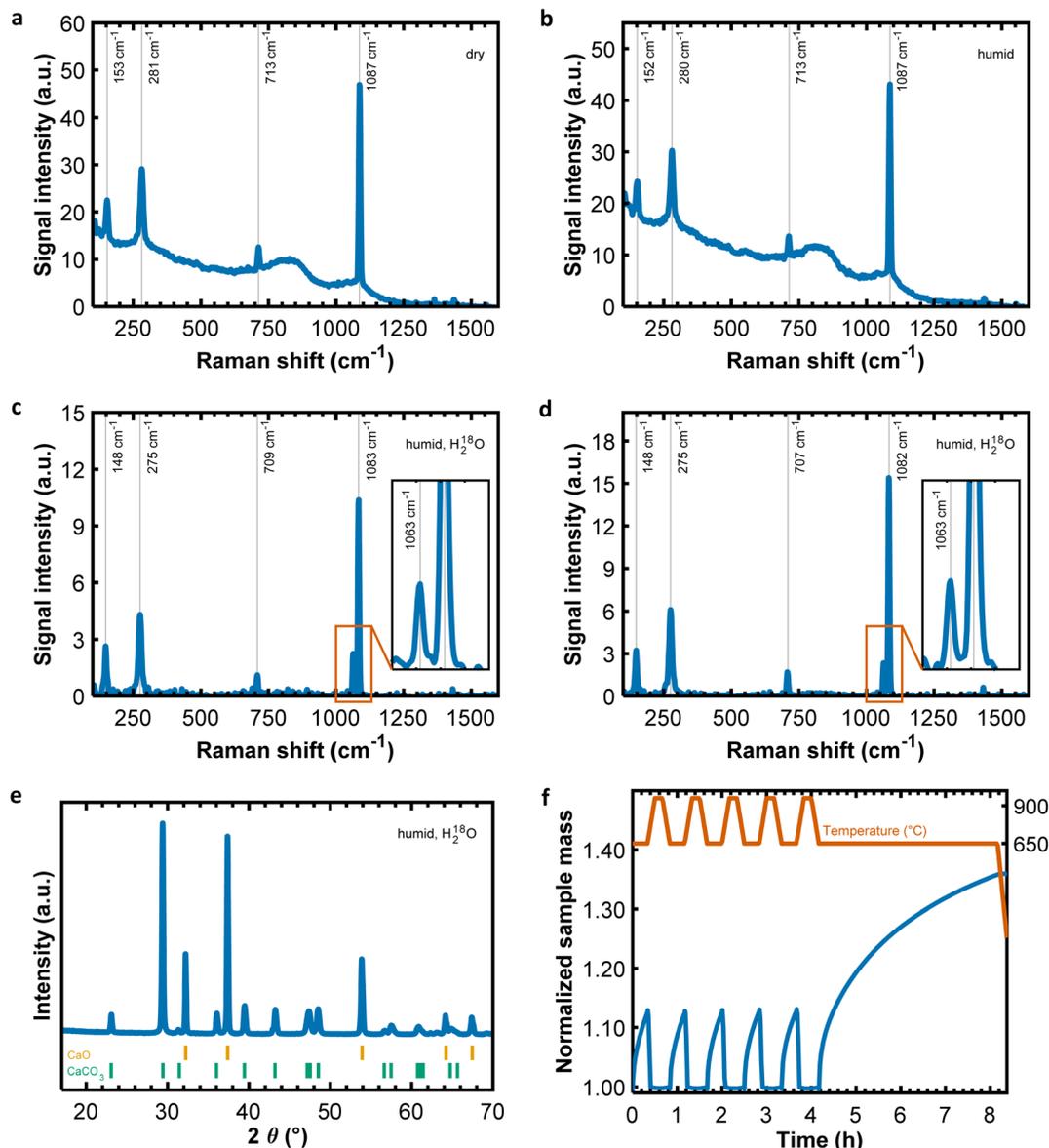
Fig. 3 (a)–(d) Raman spectroscopy measurements of partially carbonated sorbents after five reaction cycles plus an extended carbonation for 4 h. The order of the plots is the same as in Fig. 2c–f, corresponding to the different atmospheres during the carbonation stage (dry, humid ($H_2^{16}O$), humid ($H_2^{18}O$) with N_2 and CO_2 flowing through the saturator, and humid ($H_2^{18}O$) with only N_2 flowing through the saturator). (e) XRD measurement of a partially carbonated sorbent (using labeled water $H_2^{18}O$). (f) Example of a TGA experiment (here using deionized water $H_2^{16}O$) to produce the samples for the subsequent analyses shown in (a)–(e).

there was a rapid decrease in the signal due to CO_2 (m/z 44 and 46, seen in all of the Fig. 2c–f), followed by a slight, short increase due to the release of CO_2 from the material when the temperature approached ∼700 °C. Under humid conditions (Fig. 2d–f), the CO_2 uptake was greater, and so it took slightly longer to release all CO_2 captured during the subsequent heating step in dry N_2 (this is seen also from the mass changes in Fig. 2a and b). Interestingly, when steam was present during the CO_2 sorption stage at 650 °C, the MS signals due to steam (m/z 18 and 20) did not return to zero immediately after the atmosphere had been changed back to dry N_2, and even increased slightly with increasing temperature (this is seen best in the inset of Fig. 2d for m/z 18 or in Fig. 2f for m/z 20). Blank

measurements without any sample in the crucible show similar trends (Fig. 5a and b), implying that the slow decrease of the MS signals due to steam (m/z 18 and 20) when changing the atmosphere back to dry N_2 was related to the experimental setup rather than any material-related effects. Importantly, the MS signals in Fig. 2e and f show the release of CO_2 containing ^{18}O during the CO_2 release stage ($C^{16}O^{18}O$, m/z 46), indicating that a substantial amount of $CaCO_3$ containing one ^{18}O had formed during the previous carbonation stage in the presence of $H_2^{18}O$ (note the difference in magnification of m/z 46 compared to Fig. 2d). At first sight, this observation would confirm that steam indeed participates actively in the formation of $CaCO_3$, as discussed in the introduction.
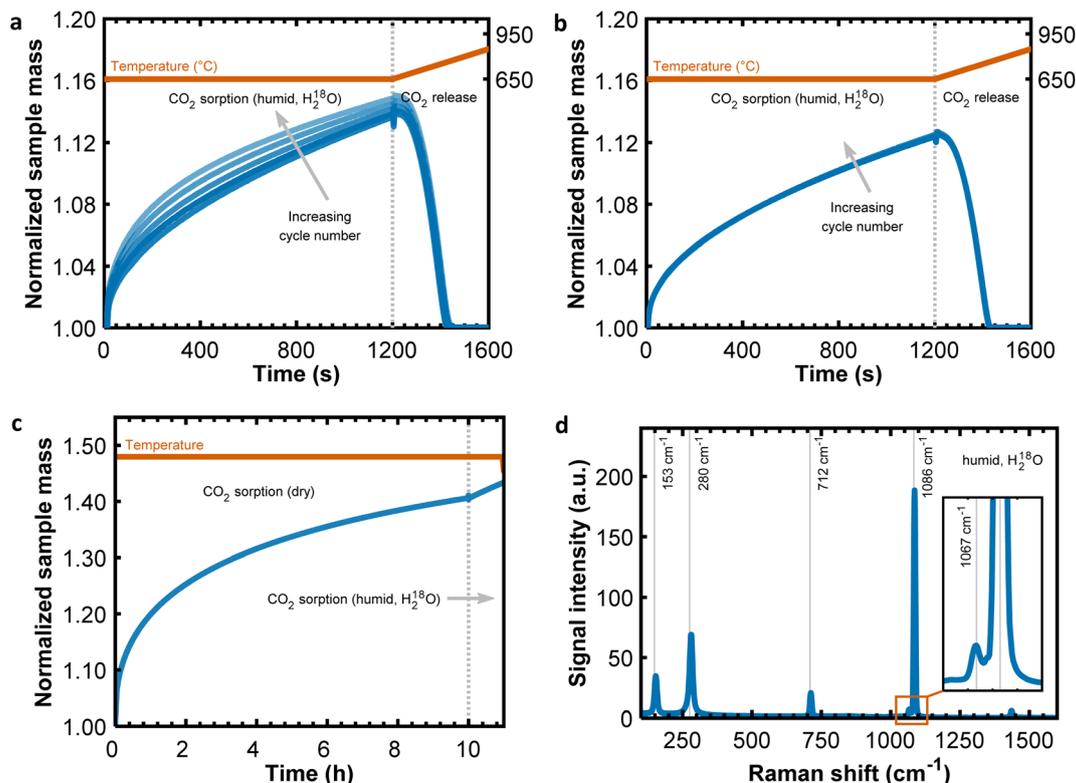
Fig. 4 Results from TGA experiments of CO_2 sorption and release using a limestone-based sorbent. (a) CO_2 sorption in a humid CO_2-containing atmosphere using steam derived labeled water ($H_2^{18}O$) with both N_2 and CO_2 flowing through the saturator. (b) CO_2 sorption in a humid CO_2-containing atmosphere using labeled water ($H_2^{18}O$) with only N_2 flowing through the saturator, two cycles only. (c) Long CO_2 sorption under dry conditions at 650 °C; after 10 h CO_2 sorption continued using steam derived from labeled water ($H_2^{18}O$), showing an increase in the rate of CO_2 uptake. (d) Raman spectroscopy measurements of the sample shown in (c).

3.2 Oxygen exchange between steam and carbon dioxide at elevated temperature

However, the release of CO_2 containing ^{18}O ($C^{16}O^{18}O$, m/z 46) is not sufficient to confirm the participation of steam in the formation of calcium carbonate, because the origin of ^{18}O is not clear yet. From control experiments (Fig. 6) and literature reports for $CaCO_3$ (ref. 38) and $MgCO_3$,[39] there is no indication that oxygen of crystalline $CaCO_3$ would be exchanged with ^{18}O contained in gas-phase H_2O or CO_2 that would have resulted in the formation $CaC^{18}O^{16}O_2$. However, although almost pure labeled water (>97 atom% ^{18}O) was used in the measurements shown in Fig. 2e and f, the intensity of m/z 18 (due to $H_2^{16}O$) was significantly greater than the intensity of m/z 20 (due to $H_2^{18}O$). Similarly, the intensity of m/z 46 (due to $C^{16}O^{18}O$) relative to m/z 44 (due to $C^{16}O_2$, for simplicity written as CO_2) during the CO_2 sorption stage was greater than expected from Table 1 or Fig. 2c and d, suggesting that ^{18}O was exchanged between the $H_2^{18}O$ and CO_2 in the reaction chamber of the TGA before interacting with the sorbent. A comparison of the MS signals (in particular the ratio m/z 46/20) in Fig. 2e (mixing of CO_2 and $H_2^{18}O$ in the saturator) and Fig. 2f (mixing of CO_2 and $H_2^{18}O$ in the gas phase downstream of the saturator just before entering the reaction chamber of the TGA) hints that the mixing of CO_2 and $H_2^{18}O$ in the gas phase led to a slightly stronger oxygen exchange/scrambling (m/z 46/20 ≈ 26, compared to m/z 46/20 ≈ 20 for

the mixing of CO_2 and $H_2^{18}O$ in the saturator). The ratio m/z 44/46 was ~10 and agreed reasonably well with the ratio of the nominal concentrations of CO_2 (15 vol%) and $H_2^{18}O$ (~1.6 vol%) in these experiments when most of the ^{18}O has been exchanged between $H_2^{18}O$ and CO_2. The initial peak of m/z 44 when switching from pure N_2 to 15 vol% CO_2/N_2 at the beginning of the CO_2 sorption stage was due to a short overshoot of the CO_2 flow rate when activating the mass flow controller (Fig. 2c–f). A corresponding spike in m/z 46 due to oxygen exchange (not due to the natural appearance of m/z 46 in CO_2, as seen in Fig. 2c, d and Table 1) was observed only when CO_2 and $H_2^{18}O$ mixed in the saturator, because slightly more $H_2^{18}O$ was taken up by the larger flow of gas (Fig. 2e), but not when CO_2 and $H_2^{18}O$ mixed in the gas phase (Fig. 2f).

Interestingly, there was hardly any signal due to m/z 48 in any of the experiments shown in Fig. 2a–f, suggesting that the ^{18}O in $H_2^{18}O$ was exchanged with only one of the two ^{16}O atoms in CO_2; for $C^{18}O_2$ to form through exchange reactions with $H_2^{18}O$, multiple collisions of the same CO_2 molecule with $H_2^{18}O$ would have been required that are unlikely given the plug flow-type gas flow pattern in the reaction chamber of the TGA (Fig. 1). This is reflected also in the Raman spectra of the carbonated samples in Fig. 3 (collected after 5 cycles plus an additional carbonation for 4 h to enhance the signal intensity due to CO_3^{2-} species, shown exemplarily in Fig. 3f). The samples carbonated under dry or humid ($H_2^{16}O$) conditions showed the most dominant
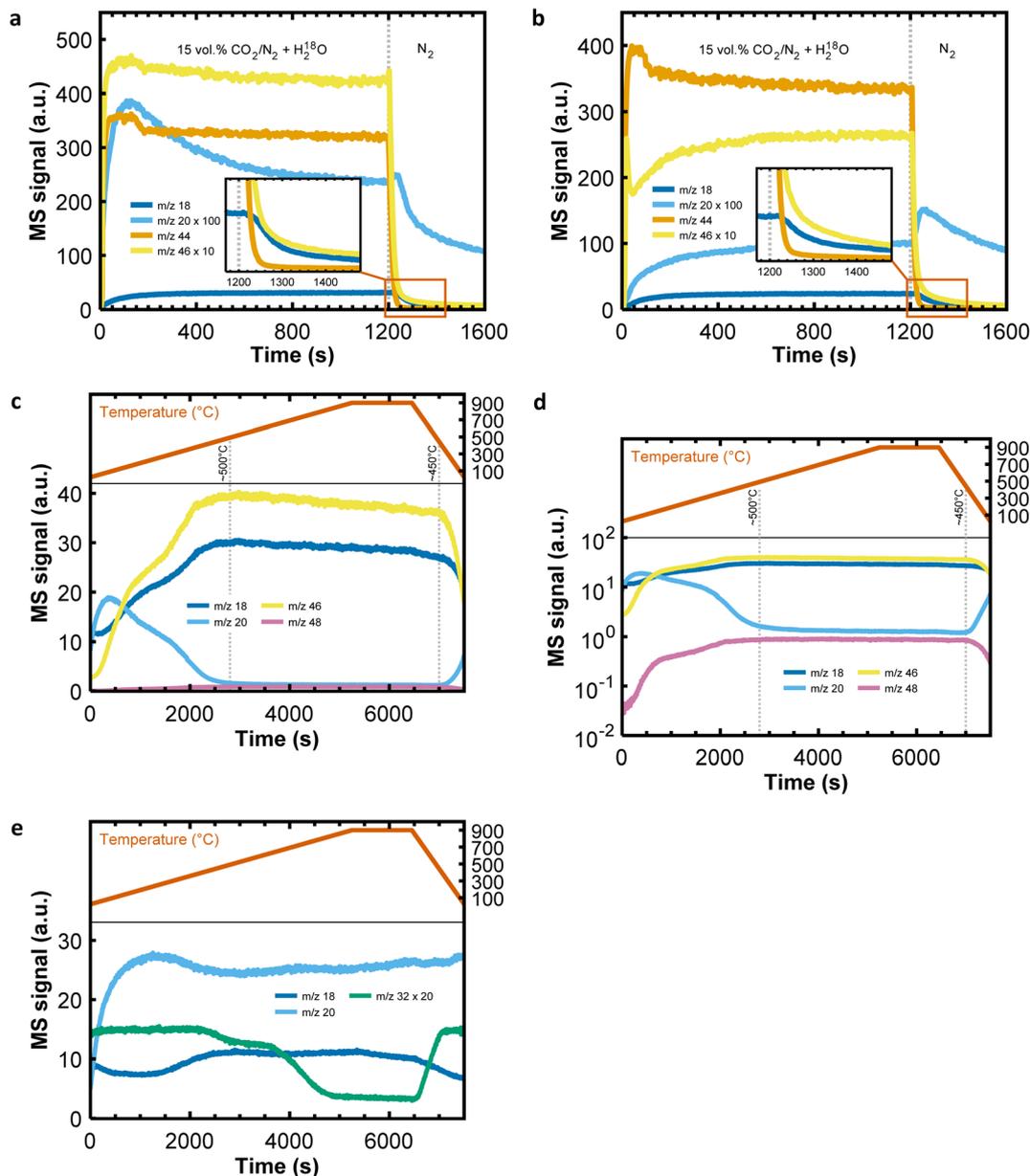
Fig. 5 Blank measurements (empty crucible) using the TGA-MS. (a) and (b) Show the MS signals corresponding to the experimental conditions in Fig. 2; in (a) both N_2 and CO_2 flowed through the saturator filled with labeled water ($H_2^{18}O$), whereas in (b) only N_2 flowed through the saturator. (c) and (d) MS signals showing the influence of temperature on the exchange of oxygen between H_2O and CO_2 when feeding a mixture of steam derived from labeled water ($H_2^{18}O$) and CO_2; in (c) the MS signals are plotted on a linear scale, whereas in (d) the MS signals are plotted on a logarithmic scale. (e) Influence of temperature on the stability of the MS signals due to water (m/z 18 and m/z 20) in the absence of CO_2; here, pure N_2 flowed through the saturator filled with a mixture of deionized water and labeled water ($H_2^{18}O$).

bands due to the ν_1 (~1087 cm^{-1}), ν_4 (~713 cm^{-1}), ν_{13} (~281 cm^{-1}) and ν_{14} (~153 cm^{-1}) vibrational modes of CO_3^{2-} species (Fig. 3a and b). The corresponding bands for the samples carbonated under humid conditions using $H_2^{18}O$ were red shifted slightly, and an additional peak due to ^{18}O replacing one of the three ^{16}O atoms in the carbonate group was observed (ν_1 vibration, ~1063 cm^{-1}, Fig. 3c and d). Additional peaks near ~1050 cm^{-1} and ~1030 cm^{-1} would have been observed had more than one ^{18}O in the carbonate group been replaced;[41] the absence (or presence below the detection limit) of these peaks agrees well with the insignificance of the MS signal m/z 48 (see

control experiments in Fig. 5c and d). The XRD pattern in Fig. 3e confirms that the partially carbonated samples consisted of unconverted CaO and the calcite phase of $CaCO_3$ only, but not any other polymorph of $CaCO_3$ (*e.g.*, aragonite or vaterite), which might have produced similar additional ν_1 vibrations as the ^{18}O in the carbonate group.[40] Considering that the sorbent was exposed to no more than ~1.5–2 vol% $C^{16}O^{18}O$ (assuming an extreme case in which all ^{18}O of $H_2^{18}O$ was exchanged with ^{16}O in CO_2) and ~13–13.5 vol% $C^{16}O_2$, it is interesting to note that the ratio of the peak areas due to $CaCO_3$ with zero ^{18}O ($CaC^{16}O_3$ at ~1087 cm^{-1}) to $CaCO_3$ with one ^{18}O ($CaC^{18}O^{16}O_2$ at

$\sim 1063 \text{ cm}^{-1}$) was $\sim$four, *i.e.*, much lower than expected from the CO_2 isotope composition in the gas stream.

3.3 Implications for the goal of this study to understand the role of steam

The exchange of oxygen between $H_2^{18}O$ and CO_2 in the reaction chamber of the TGA is a problem for the examination of the promotional mechanism of steam for the carbonation reaction, because the presence of ^{18}O in the $CaCO_3$ formed (or the release of ^{18}O-containing CO_2 from the material upon decomposition) cannot be attributed solely to a reaction mechanism that involves steam (or its oxygen component); in fact, it is much more likely that the presence of ^{18}O in $CaCO_3$ (as observed by Raman spectroscopy in Fig. 3c and d) originated from $C^{16}O^{18}O$ rather than the remaining small quantity of $H_2^{18}O$ in the gas stream. Fig. 5c shows that the exchange of oxygen between $H_2^{18}O$ (here only $\sim$0.1 vol% due to the dilution of $H_2^{18}O$ with $H_2^{16}O$ (5 : 95) in the saturator) and CO_2 (15 vol%) is temperature-dependent, and with increasing temperature, more oxygen was exchanged between the two.[42] Above $\sim$500 °C the ratios of the MS signals due to steam (*m/z* 18 and 20) and CO_2 (*m/z* 44, 46 and 48) remained constant. From Fig. 5e it is apparent that in the absence of ^{16}O-containing gas species there

was no significant change in the intensity of the MS signal due to *m/z* 20. Traces of O_2 present in N_2 ($\sim$80 ppm, *m/z* 32) appear to have exchanged ^{16}O with $H_2^{18}O$, but *m/z* 34 or *m/z* 36 were not measured in this experiment to confirm this observation.

Interestingly, the ratio *m/z* $18/20 \approx 22$ above 500 °C (Fig. 5c) was an order of magnitude lower than $\sim$330 expected from Table 1 when assuming that ^{18}O from $H_2^{18}O$ is exchanged to the level of its natural abundance in water; the short residence time (a few seconds) of the gas molecules in the high-temperature reaction chamber of the TGA may possibly have prevented an even higher degree of oxygen exchange to reach isotopic equilibrium. The lack of significant back-mixing in the reaction chamber of the TGA (as opposed to a closed system such as an autoclave), the fast rate of oxygen exchange above 500 °C, and the short gas residence time may have resulted in the exchange of only one ^{16}O in the CO_2 molecule by $H_2^{18}O$. The MS signal due to *m/z* 48 followed the same trend as *m/z* 46 (this is seen best when Fig. 5c is plotted on a logarithmic scale, Fig. 5d), indicating that indeed for a small fraction of CO_2 molecules entering the reaction chamber of the TGA both ^{16}O atoms in the CO_2 molecule were exchanged by two different $H_2^{18}O$ molecules; however, the high ratio *m/z* $46/48 \approx 42$ shows that the exchange of only one oxygen atom in the CO_2 molecule with $H_2^{18}O$ was dominant.
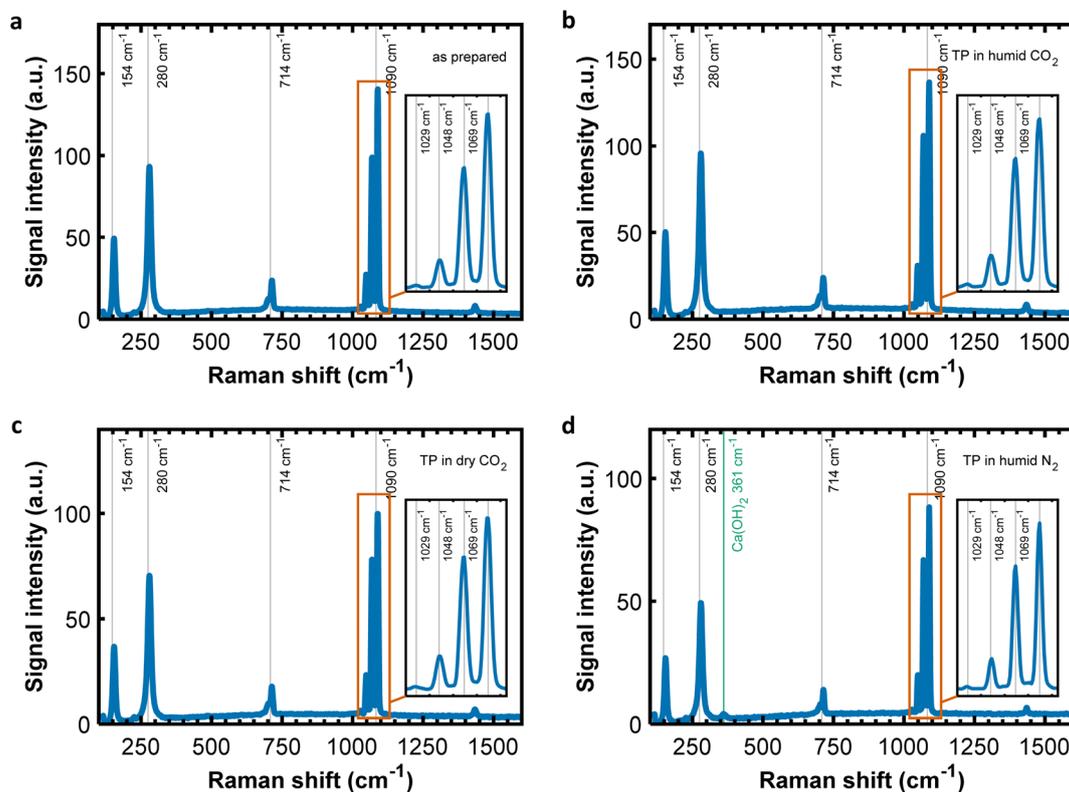

Fig. 6 Raman spectroscopy measurements of partially carbonated sorbents following a temperature–programmed (TP) treatment in a larger TGA under different conditions. (a) The partially carbonated sorbent was prepared by calcining $CaCO_3$ powder at 900 °C, followed by exposure to 5 vol% CO_2 and 2 vol% steam derived from labeled water ($H_2^{18}O$) at 700 °C for 12 h. The CO_2 uptake was 0.75 g CO_2 per g sorbent. (b) The material prepared in (a) was heated from room temperature to 600 °C in 5 vol% CO_2 and 2 vol% steam derived from deionized water. (c) The material prepared in (a) was heated from room temperature to 600 °C in 5 vol% CO_2. (d) The material prepared in (a) was heated from room temperature to 600 °C in 2 vol% steam derived from deionized water. Ratio of peak areas ($CaC^{16}O_3$ at 1090 cm^{-1} and $CaC^{18}O^{16}O_2$ at 1069 cm^{-1}): 1.4 (a), 1.3 (b), 1.3 (c) and 1.3 (d).

For completeness, we performed an additional series of experiments using a TGA with a larger reaction chamber (∼46 ml) to facilitate back-mixing of the reaction gas, and thereby enhance the probability of oxygen exchange between H_2O and CO_2 molecules. Commercial $CaCO_3$ powder (extra pure, Fisher Scientific) was calcined at 900 °C in N_2, followed by carbonation at 700 °C in steam (∼2 vol%, derived from labeled water) and CO_2 (∼5 vol%) for 12 h. Indeed, Raman spectroscopy revealed additional features of the ν_1 vibration (Fig. 6a), indicating that the partially carbonated sorbent contained, in addition to the experiments performed in the smaller TGA, two and three ^{18}O in the carbonate group.[40] Upon further treatment of the material in atmospheres without ^{18}O, there was no noticeable change in the ratio of peak areas in the ν_1 region ($CaC^{16}O_3$ at 1090 cm^{-1} and $CaC^{18}O^{16}O_2$ at 1069 cm^{-1}), Fig. 6a–c. Thus, no measurable oxygen exchange occurred between gaseous CO_2 and, or, H_2O and the solid $CaCO_3$ over the timescale and conditions of our experiments (for comparison see *e.g.*, the work by Rosenbaum[34] who has reported carbon and oxygen isotope exchange for CO_2 and $CaCO_3$ at 900 °C). The material treated in H_2O/N_2 decomposed slightly, explaining an additional Raman band due to $Ca(OH)_2$ in Fig. 6d. Interestingly, the small peak at 1029 cm^{-1} in Fig. 6a–c originated from $CaCO_3$ containing three ^{18}O ($CaC^{18}O_3$). Since oxygen exchange between $H_2^{18}O$ and CO_2 in the high-temperature reaction chamber of the larger TGA yielded, at best, $C^{18}O_2$, a mixture of $CaC^{18}O_2^{16}O$, $CaC^{18}O^{16}O_2$ and $CaC^{16}O_3$ would be expected upon reaction with CaO. Thus, the results from Raman spectroscopy indicate that there must have been additional oxygen exchange between ^{18}O-containing H_2O or CO_2 and the solid phases CaO or $CaCO_3$. With CO_3^{2-} diffusing through the $CaCO_3$ product layer toward the CaO–$CaCO_3$ interface,[24] oxygen (and carbon) exchange would be expected as part of the volume/lattice diffusion mechanism (involving possibly recrystallization or Ostwald ripening),[34,43,44] but this was not observed in our experiments (Fig. 6a–c) and therefore ruled out as an explanation for the formation of $CaC^{18}O_3$. Given the relatively fast rates of carbonation under both dry and humid conditions (Fig. 2a and b), it is unlikely that volume/lattice diffusion was rate-controlling in our experiments.[45] Instead, diffusion along grain boundaries or narrow pores (note that $CaCO_3$ crystals formed during carbonation are far from perfect[46]) may have dominated mass transport,[47] decreasing the likelihood of oxygen exchange between CO_2/CO_3^{2-} and $CaCO_3$.[26] It is thus possible that the presence of three ^{18}O in $CaCO_3$ originates from oxygen exchange with CaO. CO_2 would immediately form $CaCO_3$ when in contact with CaO, implying that H_2O is responsible for the exchange of oxygen with CaO that results in the formation of $CaC^{18}O_3$ upon further reaction with $C^{18}O_2$. Similar results have been reported previously, suggesting that steam can interact with CaO above the decomposition temperature of $Ca(OH)_2$.[38] Whether the oxygen exchange between steam and CaO under reaction conditions contributes to the accelerated rates of CO_2 uptake remains, however, uncertain but may motivate future research activities. The presence of steam alters the dominant transport mechanism of species required to form $CaCO_3$ (*viz.* carbon and oxygen),[48] but its identification and quantification is difficult

due to the challenging reaction conditions and the relatively short timescale of the carbonation reaction. From the absence of measurable oxygen exchange between H_2O or CO_2 and $CaCO_3$ we conclude that volume/lattice diffusion appears to play a negligible role in the carbonation reaction using limestone-derived particles, and therefore many mechanisms discussed in the literature such as the hydrolyzation and weakening of C–O bonds in $CaCO_3$ through protons, or the faster OH$^-$ diffusion over O^{2-} diffusion through $CaCO_3$ may not apply under relevant reaction conditions.

Investigations of oxygen isotope exchange may not be suited to unveil the enhancement effect of steam during the carbonation of CaO at high temperatures, as there will always be oxygen exchange between the gaseous oxygen-containing reactants. The intrinsic properties of steam causing the acceleration of CO_2 uptake cannot be linked with the oxygen or hydrogen components, and oxygen atoms originating from the water molecule will inevitably end up in the $CaCO_3$ product through different sequences of oxygen exchange. However, our experiments did provide insights into the presence or absence of oxygen exchange between the gas and solid components involved in the carbonation reaction, from which information on the relevant transport processes can be obtained.

4. Conclusions

In calcium looping, the presence of steam is known to accelerate the rate of CO_2 uptake. We designed experiments in which steam derived from labeled water ($H_2^{18}O$) was used to promote CO_2 sorption in a TGA, and tracked ^{18}O in gaseous and solid products through mass spectrometry and Raman spectroscopy to obtain mechanistic insights into the enhancement effect, for example whether oxygen contained in steam contributes directly to carbonate formation. While we indeed observed the incorporation of ^{18}O into the calcite structure (and the release of ^{18}O-containing CO_2 in the subsequent decomposition step), we found that most of ^{18}O contained in labelled water was exchanged with ^{16}O contained in CO_2 in the high-temperature reaction chamber of the TGA before reaching the sorbent. Thus, the CO_2 contained a substantial fraction of ^{18}O before reacting with CaO to form $CaCO_3$ that contained ^{18}O. The degree of oxygen exchange between H_2O and CO_2 depended greatly on temperature, but also the contact time and the gas flow pattern in the high-temperature reaction chamber of the TGA. With the given reaction conditions and our experimental setup, it was not possible to eliminate oxygen exchange between H_2O and CO_2 completely. Using a larger TGA furnace facilitated back-mixing of gas and increased its residence time in the TGA, which in turn enhanced the degree of oxygen exchange such that not only $C^{18}O^{16}O$ but also $C^{18}O_2$ was formed. Consequently, Raman spectroscopy revealed the formation of $CaCO_3$ with zero, one, two and three ^{18}O atoms in the carbonate group.

Although the use of labelled water/steam was not suitable under the given reaction conditions to obtain unequivocal insight into why steam accelerates CO_2 uptake, oxygen interactions between solid and gas phases could be probed. Our results indicate that there is no oxygen exchange between solid

CaCO$_3$ and H$_2$O/CO$_2$ under reaction conditions relevant to calcium looping. However, oxygen exchange appears to occur between solid CaO and H$_2$O, which may contribute to the enhancement effect of steam, and motivate further investigations.

Conflicts of interest

There are no conflicts to declare.

Data availability

All data presented in Fig. 2–6 is available through the Zenodo repository (10.5281/zenodo.17395250).

References

1 J. Chen, L. Duan and Z. Sun, Review on the Development of Sorbents for Calcium Looping, *Energy Fuels*, 2020, **16**, 7806–7836, DOI: 10.1021/acs.energyfuels.0c00682.

2 C. Wu, Q. Huang, Z. Xu, A. T. Sipra, N. Gao, L. P. d. S. Vandenberghe, S. Vieira, C. R. Soccol, R. Zhao and S. Deng, *et al.*, A Comprehensive Review of Carbon Capture Science and Technologies, *Carbon Capture Science and Technology*, Elsevier Ltd, 2024, DOI: 10.1016/j.ccst.2023.100178.

3 M. T. Dunstan, F. Donat, A. H. Bork, C. P. Grey and C. R. Müller, CO2 Capture at Medium to High Temperature Using Solid Oxide-Based Sorbents: Fundamental Aspects, Mechanistic Insights, and Recent Advances, *Chem. Rev.*, 2021, **27**, 12681–12745, DOI: 10.1021/acs.chemrev.1c00100.

4 J. Moreno, M. Hornberger, M. Schmid and G. Scheffknecht, Part-Load Operation of a Novel Calcium Looping System for Flexible CO2 Capture in Coal-Fired Power Plants, *Ind. Eng. Chem. Res.*, 2021, **60**(19), 7320–7330, DOI: 10.1021/acs.iecr.1c00155.

5 J. Ströhle, J. Hilz and B. Epple, Performance of the Carbonator and Calciner during Long-Term Carbonate Looping Tests in a 1 MWth Pilot Plant, *J. Environ. Chem. Eng.*, 2020, **8**(1), DOI: 10.1016/j.jece.2019.103578.

6 B. Arias, Y. Alvarez Criado, A. Méndez, P. Marqués, I. Finca and J. C. Abanades, Pilot Testing of Calcium Looping at TRL7 with CO2 Capture Efficiencies toward 99%, *Energy Fuels*, 2024, **38**(15), 14757–14764, DOI: 10.1021/acs.energyfuels.4c02472.

7 A. Otto, T. Grube, S. Schiebahn and D. Stolten, Closing the Loop: Captured CO2 as a Feedstock in the Chemical Industry, *Energy Environ. Sci.*, 2015, **8**(11), 3283–3297, DOI: 10.1039/c5ee02591e.

8 W. Gao, S. Liang, R. Wang, Q. Jiang, Y. Zhang, Q. Zheng, B. Xie, C. Y. Toe, X. Zhu, J. Wang, *et al.*, Industrial Carbon Dioxide Capture and Utilization: State of the Art and Future Challenges, *Chem. Soc. Rev.*, 2020, **7**, 8584–8686, DOI: 10.1039/d0cs00025f.

9 F. Donat, N. H. Florin, E. J. Anthony and P. S. Fennell, Influence of High-Temperature Steam on the Reactivity of CaO Sorbent for CO2 Capture, *Environ. Sci. Technol.*, 2012, **46**(2), 1262–1269, DOI: 10.1021/es202679w.

10 S. Zhang, S. He, N. Gao, C. Quan and C. Wu, Effect of Steam Addition for Energy Saving during CaCO3 Calcination of Auto Thermal Biomass Gasification, *Biomass Bioenergy*, 2022, **161**, DOI: 10.1016/j.biombioe.2022.106416.

11 J. Arcenegui-Troya, P. E. Sánchez-Jiménez, A. Perejón, V. Moreno, J. M. Valverde and L. A. Pérez-Maqueda, Kinetics and Cyclability of Limestone (CaCO3) in Presence of Steam during Calcination in the CaL Scheme for Thermochemical Energy Storage, *Chem. Eng. J.*, 2021, **417**, DOI: 10.1016/j.cej.2021.129194.

12 G. Giammaria and L. Lefferts, Catalytic Effect of Water on Calcium Carbonate Decomposition, *J. CO2 Util.*, 2019, **33**, 341–356, DOI: 10.1016/j.jcou.2019.06.017.

13 M. Silakhori, M. Jafarian, A. Chinnici, W. Saw, M. Venkataraman, W. Lipiński and G. J. Nathan, Effects of Steam on the Kinetics of Calcium Carbonate Calcination, *Chem. Eng. Sci.*, 2021, **246**, DOI: 10.1016/j.ces.2021.116987.

14 J. Arcenegui-Troya, P. E. Sánchez-Jiménez, A. Perejón, J. M. Valverde and L. A. Pérez-Maqueda, Steam-Enhanced Calcium-Looping Performance of Limestone for Thermochemical Energy Storage: The Role of Particle Size, *J. Energy Storage*, 2022, **51**, DOI: 10.1016/j.est.2022.104305.

15 J. Dong, Y. Tang, A. Nzihou and E. Weiss-Hortala, Effect of Steam Addition during Carbonation, Calcination or Hydration on Re-Activation of CaO Sorbent for CO2 Capture, *J. CO2 Util.*, 2020, **39**, DOI: 10.1016/j.jcou.2020.101167.

16 N. Rong, J. Wang, K. Liu, L. Han, Z. Mu, X. Liao and W. Meng, Enhanced CO2 Capture Durability and Mechanical Properties Using Cellulose-Templated CaO-Based Pellets with Steam Injection during Calcination, *Ind. Eng. Chem. Res.*, 2023, **62**(3), 1533–1541, DOI: 10.1021/acs.iecr.2c03746.

17 N. Rong, J. Wang, L. Han, Y. Wu, Z. Mu, X. Wan and G. Wang, Effect of Steam Addition during Calcination on CO2 Capture Performance and Strength of Bio-Templated Ca-Based Pellets, *J. CO2 Util.*, 2022, **63**, DOI: 10.1016/j.jcou.2022.102127.

18 S. Champagne, D. Y. Lu, A. MacChi, R. T. Symonds and E. J. Anthony, Influence of Steam Injection during Calcination on the Reactivity of CaO-Based Sorbent for Carbon Capture, *Ind. Eng. Chem. Res.*, 2013, **52**(6), 2241–2246, DOI: 10.1021/ie3012787.

19 L. Zhang, B. Zhang, Z. Yang and M. Guo, The Role of Water on the Performance of Calcium Oxide-Based Sorbents for Carbon Dioxide Capture: A Review, *Energy Technol.*, 2015, **3**(1), 10–19, DOI: 10.1002/ente.201402099.

20 J. Zha, Y. Yan, P. Ma, Y. Huang, F. Qi, X. Liu, R. Diao and D. Yan, The Role of Water Vapour on CO2 Mobility on Calcite Surface during Carbonation Process for Calcium Looping: A DFT Study, *Carbon Capture Sci. Technol.*, 2024, **12**, DOI: 10.1016/j.ccst.2024.100226.

21 Y. Fan, J. G. Yao, Z. Zhang, M. Sceats, Y. Zhuo, L. Li, G. C. Maitland and P. S. Fennell, Pressurized Calcium Looping in the Presence of Steam in a Spout-Fluidized-Bed Reactor with DFT Analysis, *Fuel Process. Technol.*, 2018, **169**, 24–41, DOI: 10.1016/j.fuproc.2017.09.006.

22 H. Wang, Z. Li and N. Cai, Multiscale Model for Steam Enhancement Effect on the Carbonation of CaO Particle, *Chem. Eng. J.*, 2020, **394**, DOI: 10.1016/j.cej.2020.124892.

23 Z. Li, Y. Liu and N. Cai, Understanding the Enhancement Effect of High-Temperature Steam on the Carbonation Reaction of CaO with CO2, *Fuel*, 2014, **127**, 88–93, DOI: 10.1016/j.fuel.2013.06.040.

24 Z. Sun, S. Luo, P. Qi and L. S. Fan, Ionic Diffusion through Calcite (CaCO3) Layer during the Reaction of CaO and CO2, *Chem. Eng. Sci.*, 2012, **81**, 164–168, DOI: 10.1016/j.ces.2012.05.042.

25 J. Ruan, C. Gao, T. Deng and C. Qin, Understanding the Influences and Mechanism of Water Vapor on CO2 Capture by High-Temperature Li4SiO4 Sorbents, *Sep. Purif. Technol.*, 2025, **354**, DOI: 10.1016/j.seppur.2024.129289.

26 J. R. Farver and R. A. Yund, Measurement of Oxygen Grain Boundary Diffusion in Natural, Fine-Grained, Quartz Aggregates, *Geochim. Cosmochim. Acta*, 1991, **55**, 1597–1607, DOI: 10.1016/0016-7037(91)90131-N.

27 J. R. Farver, Oxygen and Hydrogen Diffusion in Minerals, *Rev. Mineral. Geochem.*, 2010, **72**, 447–507, DOI: 10.2138/rmg.2010.72.10.

28 A. K. Kronenberg, R. A. Yund and B. J. Giletti, Carbon and Oxygen Diffusion in Calcite: Effects of Mn Content and PH2O, *Phys. Chem. Miner.*, 1984, **11**, 101–112, DOI: 10.1007/BF00309248.

29 J. R. Farver and R. A. Yund, Oxygen Diffusion in Quartz: Dependence on Temperature and Water Fugacity, *Chem. Geol.*, 1991, **90**, 55–70, DOI: 10.1016/0009-2541(91)90033-N.

30 J. R. Farver, Oxygen Self-Diffusion in Calcite: Dependence on Temperature and Water Fugacity, *Earth Planet. Sci. Lett.*, 1994, **121**, 575–587, DOI: 10.1016/0012-821X(94)90092-2.

31 Y. Zhang, E. M. Stolper and G. J. Wasserburg, Diffusion of a Multi-Species Component and Its Role in Oxygen and Water Transport in Silicates, *Earth Planet. Sci. Lett.*, 1991, **103**, 228–240, DOI: 10.1016/0012-821X(91)90163-C.

32 T. C. Labotka, D. R. Cole, M. J. Fayek and T. Chacko, An Experimental Study of the Diffusion of C and O in Calcite in Mixed CO2-H2O Fluid, *Am. Mineral.*, 2011, **96**(8–9), 1262–1269, DOI: 10.2138/am.2011.3738.

33 D. C. Brenner, B. H. Passey and D. A. Stolper, Influence of Water on Clumped-Isotope Bond Reordering Kinetics in Calcite, *Geochim. Cosmochim. Acta*, 2018, **224**, 42–63, DOI: 10.1016/j.gca.2017.12.026.

34 J. M. Rosenbaum, Stable Isotope Fractionation between Carbon Dioxide and Calcite at 900°C, *Geochim. Cosmochim. Acta*, 1994, **58**(17), 3747–3753, DOI: 10.1016/0016-7037(94)90164-3.

35 F. Donat and C. R. Müller, A Critical Assessment of the Testing Conditions of CaO-Based CO2 Sorbents, *Chem. Eng. J.*, 2018, **336**, 544–549, DOI: 10.1016/j.cej.2017.12.050.

36 NIST Mass Spectrometry Data Center. Mass Spectra, in *NIST Chemistry WebBook*, NIST Standard Reference Database Number 69, ed. Linstrom, P. J. and Mallard, W. G., National Institute of Standards and Technology, Gaithersburg MD, 2024.

37 G. S. Grasa and J. C. Abanades, CO2 Capture Capacity of CaO in Long Series of Carbonation/Calcination Cycles, *Ind. Eng. Chem. Res.*, 2006, **45**(26), 8846–8851, DOI: 10.1021/ie0606946.

38 L. Thum, M. Rudolph, R. Schomäcker, Y. Wang, A. Tarasov, A. Trunschke and R. Schlögl, Oxygen Activation in Oxidative Coupling of Methane on Calcium Oxide, *J. Phys. Chem. C*, 2019, **123**(13), 8018–8026, DOI: 10.1021/acs.jpcc.8b07391.

39 A. Landuyt, P. V. Kumar, J. A. Yuwono, A. H. Bork, F. Donat, P. M. Abdala and C. R. Müller, Uncovering the CO2 Capture Mechanism of NaNO3-Promoted MgO by 18O Isotope Labeling, *JACS Au*, 2022, **2**(12), 2731–2741, DOI: 10.1021/jacsau.2c00461.

40 M. De La Pierre, C. Carteret, L. Maschio, E. André, R. Orlando and R. Dovesi, The Raman Spectrum of CaCO3 Polymorphs Calcite and Aragonite: A Combined Experimental and Computational Study, *J. Chem. Phys.*, 2014, **140**(16), DOI: 10.1063/1.4871900.

41 P. Gillet, P. McMillan, J. Schott, J. Badro and A. Grzechnik, Thermodynamic Properties and Isotopic Fractionation of Calcite from Vibrational Spectroscopy of 18O-Substituted Calcite, *Geochim. Cosmochim. Acta*, 1996, **60**(18), 3471–3485, DOI: 10.1016/0016-7037(96)00178-0.

42 G. Chiodini, P. Allard, S. Caliro and F. Parello, 18O Exchange between Steam and Carbon Dioxide in Volcanic and Hydrothermal Gases: Implications for the Source of Water, *Geochim. Cosmochim. Acta*, 2000, **64**(14), 2479–2488, DOI: 10.1016/S0016-7037(99)00445-7.

43 D. R. Cole and S. Chakraborty, Rates and Mechanisms of Isotopic Exchange, *Rev. Mineral. Geochem.*, 2001, **43**(1), 83–223, DOI: 10.2138/gsrmg.43.1.83.

44 T. Chacko, T. K. Mayeda, R. N. Clayton and J. R. Goldsmith, Oxygen and Carbon Isotope Fractionations between CO2 and Calcite, *Geochim. Cosmochim. Acta*, 1991, **55**, 2867–2882, DOI: 10.1016/0016-7037(91)90452-B.

45 M. Krödel, D. Spescha, A. Kierzkowska, F. Donat and C. R. Müller, Experimental and Numerical Investigation of the Morphological Changes of a Natural Limestone-Based CO2 Sorbent over Repeated Carbonation-Calcination Cycles, *Carbon Capture Sci. Technol.*, 2025, **16**, 100486, DOI: 10.1016/j.ccst.2025.100486.

46 D. Mess, A. F. Sarofim and J. P. Longwell, Product Layer Diffusion during the Reaction of Calcium Oxide with Carbon Dioxide, *Energy Fuels*, 1999, **13**(5), 999–1005, DOI: 10.1021/ef980266f.

47 J. R. Farver and R. A. Yund, Oxygen Grain Boundary Diffusion in Natural and Hot-Pressed Calcite Aggregates, *Earth Planet. Sci. Lett.*, 1998, **161**, 189–200, DOI: 10.1016/S0012-821X(98)00150-2.

48 J. R. Farver and R. A. Yund, Oxygen Diffusion in a Fine-Grained Quartz Aggregate with Wetted and Nonwetted Microstructures, *J. Geophys. Res.*, 1992, **97**(B10), 14017–14029, DOI: 10.1029/92jb01206.